HHS Public Access

Author manuscript

J Orthop Res. Author manuscript; available in PMC 2019 January 01.

Published in final edited form as:

J Orthop Res. 2018 January ; 36(1): 183–191. doi:10.1002/jor.23622.

Near Infrared Spectroscopy for Measuring Changes in Bone Hemoglobin Content after Exercise in Individuals with Spinal Cord Injury

Adina E. Draghici[1], **Diane Potart**[2], **Joseph L. Hollmann**[3], **Vivian Pera**[4], **Qianqian Fang**[1,5], **Charles A. DiMarzio**[5], **J. Andrew Taylor**[6,7], **Mark J. Niedre**[1,5], and **Sandra J. Shefelbine**[1,8]

[1]Department of Bioengineering, Northeastern University, Boston, MA, USA

[2]Université de Technologie Compiègne, Compiègne, France

[3]ICFO – Institut de Ciencies Fotoniques, Barcelona, Spain

[4]Department of Biomedical Engineering, Boston University, Boston, MA, USA

[5]Department of Electrical and Computer Engineering, Northeastern University, Boston, MA, USA

[6]Cardiovascular Research Laboratory, Spaulding Rehabilitation Hospital, Cambridge, MA, USA

[7]Department of Physical Medicine and Rehabilitation, Harvard Medical School, Boston, MA, USA

[8]Department of Mechanical and Industrial Engineering, Northeastern University, Boston, MA, USA

Abstract

Bone blood perfusion has an essential role in maintaining a healthy bone. However, current methods for measuring bone blood perfusion are expensive and highly invasive. This study presents a custom built near-infrared spectroscopy (NIRS) instrument to measure changes in bone blood perfusion. We demonstrated the efficacy of this device by monitoring oxygenated and deoxygenated hemoglobin changes in the human tibia during and after exercise in able-bodied and in individuals with spinal cord injury (SCI), a population with known impaired peripheral blood perfusion. Nine able-bodied individuals and six volunteers with SCI performed a 10 minutes rowing exercise (functional electrical stimulation rowing for those with SCI). With exercise, during rowing, able-bodied showed an increase in deoxygenated hemoglobin in the tibia. Post rowing, able-bodied showed an increase in total blood content, characterized by an increase in total hemoglobin content due primarily to an increase in deoxygenated hemoglobin. During rowing and post-rowing, those with SCI showed no change in total blood content in the tibia. The current study demonstrates that NIRS can non-invasively detect changes in hemoglobin concentration in the tibia.

Corresponding author: Adina E. Draghici, Department of Bioengineering, Northeastern University, 260 Egan Research Center, 360 Huntington Ave, Boston, MA 02115, draghici.a@husky.neu.edu.

All authors contributed extensively to the work presented in this paper. A.E.D., D.P. M.J.N. and S.J.S. designed the experiment and discussed the results and implications at all stages. A.E.D. analyzed the results and wrote the manuscript. D.P. collected data. J.L.H. and C.A.D. provided technical support and helped developing the device. V.P. and Q.F. helped develop the analytical tools. All authors critically revised the manuscript and approved the final version of the submitted manuscript

Keywords

bone blood perfusion; near infrared spectroscopy; exercise; spinal cord injury; hemoglobin content

Introduction

Bone is a highly vascular tissue, and bone blood circulation has a critical role in nutrient delivery and oxygen consumption, thereby influencing bone metabolic activity. Moreover, bone blood flow plays an active role in controlling the osteogenesis process [1]. An intact vascular network is necessary for all skeletal processes, including growth, repair, maintenance, and remodeling [2–6]. Changes in blood perfusion to bone may indicate a pathophysiological process. For example, increased bone blood perfusion results from cancers, hyper-remodeling, osteoarthritis, and bone marrow lesions; whereas decreased perfusion is associated with osteonecrosis, osteoporosis, and fracture non-union [7–9].

Though the importance of blood flow in bone is clear, it remains poorly studied. The dense nature of bone makes it very difficult to investigate blood circulation and the techniques used to quantify circulation in other tissues are either difficult or impossible to apply to bone *in vivo*. The current "gold standard" for measuring bone blood flow is the radioactive microsphere technique. However, this technique is highly invasive, requiring the use of radioactively labeled particles and sampling of tissues, making it inappropriate for clinical measurements [10–12]. Positron emission tomography, ultrasound Doppler velocimetry, intraoperative measurement of oxygen tension and MRI provide an indication of perfusion with limitations of radiation, invasiveness (use of contrast agents), difficulty in quantifying bone blood flow, and high cost.

Near infra-red spectroscopy (NIRS) is commonly used to assess blood perfusion in soft tissue [13–17]. NIRS relies on spectral differences in the light absorbing properties of oxygenated (O_2Hb) and deoxygenated (HHb) hemoglobin to determine a quantitative measure of oxygenation saturation and hemoglobin content in tissue. NIRS, however, has not been extensively used to assess blood perfusion in bone. A few studies have used optical approaches to measure blood perfusion in bone marrow, which is clinically significant for marrow cancers.[18–22] These studies have shown that NIRS can measure the effects of physiological events on blood perfusion (microgravity[18], orthostatic stress [19], aging [21]). NIRS was also used to assess pulsatile flow in the patella[23,24]. Aziz *et al.*[22] presented hemoglobin content in tibia cortical bone in a single individual during cuff inflation using a NIRS instruments developed specifically for bone. Sekar *et al.*[25] used time-resolved diffuse optical spectroscopy to probe bone oxygen consumption and blood flow in different superficial bones in able-bodied individuals. These promising results indicate the potential of optical techniques in investigating blood content in bone.

In this study, we use NIRS to assess physiological changes in blood content in cortical bone. The main objective of this study was to apply NIRS to measure changes in hemoglobin concentration in tibial cortical bone during and after exercise. Tibial bone was chosen for NIRS monitoring because it is an easily accessible superficial bone. Previous studies indicate that regional bone blood flow increases during and directly after a period of

physical exercise in humans[26] (measured with PET) and rats[27] (measured with radiolabeled microspheres). Therefore, we hypothesized that NIRS measurements would indicate an increase in the amount of blood in bone immediately after exercise in an able-bodied population.

A second objective was to determine if our sensor was sensitive enough to measure differences in hemoglobin concentration in a population with impaired blood perfusion, namely the spinal cord injury (SCI) population. Pilot work (in conference proceedings[28,29]) has presented methods of using NIRS in those with SCI, but results of the full studies have not been reported. A spinal cord lesion results in a reduction in blood flow in the regions below the level of injury [30–33], and individuals with complete SCI have greater blood flow impairment compared to those with incomplete SCI [32]. Additionally, the lack of muscle contraction of the legs resulting in a loss of mechanical loading of the bone further contributes to a possible abnormal peripheral bone blood flow circulation. Thus, we used NIRS to assess bone blood perfusion in the SCI population before and after functional electrical stimulation (FES) assisted rowing. This uses electrical stimulation to produce hamstrings and quadriceps contractions, allowing for flexion and extension of the knee [34–36]. While an increase in bone blood perfusion with exercise is expected in the able-bodied, it is unknown how exercise affects blood perfusion in the bone in those with SCI. We hypothesized that those with SCI would have smaller changes in hemoglobin concentration in the tibia during exercise compared to the able-bodied population due to impaired peripheral blood perfusion.

Methods

Experimental Apparatus

A custom NIRS system was developed to monitor oxygenated and deoxygenated hemoglobin changes in the human tibia bone as shown in Figure 1. The major differences between our system and commercially available systems frequently used in assessing hemoglobin changes in muscle [37,38] are: 1) we have two detector locations as opposed to one, which allows us to estimate hemoglobin changes in a two-layer (skin and bone) model, as opposed to a single homogenous medium, and 2) we use a broadband light source and high-sensitivity spectrometers to yield full NIR spectral information, as opposed to making measurements at only two wavelengths. Specifically, the instrument used a white-light tungsten halogen lamp (Fostec DCRII, Dallas, TX, USA) to deliver light through a large optical fiber bundle to the skin. We used two detector fibers coupled to spectrometers (Mini-spectrometer TG C9405CB, Hamamatsu Photonics, Japan), placed at 1 cm and 2 cm distances (center-to-center) from the source. Both spectrometers allowed us to measure the diffusely reflected light between 650 nm and 800 nm with 5 nm resolution. The light source and the two detectors were attached to a custom made probe head that was placed on the skin surface directly over the tibia. Light propagates between the source and the detectors in “banana-shaped” sensitivity functions [13,14,16]. It is a property of light propagation in biological tissue that light penetrates shallower for more closely separated source-detector pairs and more deeply for wider separated pairs. Therefore, the detector 1 cm from the source (detector A) primarily probed the relatively thin (2 mm) skin layer with some

contribution from the bone. The detector 2 cm from the source (detector B) probed deeper into tissue and was therefore more sensitive to the underlying bone. To minimize the effects of soft tissue (muscle) and a local increase in skin blood flow with exercise on the NIRS measurements, the probe head was placed on the anterior side of the tibia where the bone lies directly under the skin.

Validation of NIRS device

NIRS has been previously used to detect changes in blood flow in muscle during voluntary contractions [26,38–40]. To validate that our device could detect changes in blood in soft tissue (before applying it to bone), we analyzed changes in blood perfusion in the quadriceps muscle during an isometric contraction. An able-bodied individual performed maximal and submaximal quadriceps voluntary contractions using a Biodex Isokinetic dynamometer (Biodex). The hip was fixed to the dynamometer by a strap and the knee joint angle was flexed at 125° (180° is fully extended). The ankle joint was attached to a bar linked to the force transducer. During contraction, the subject was asked to exert force by knee extension action and to fold the arms across the chest. The subject was asked to perform 2 voluntary contractions, a submaximal contraction at ~30% of the maximum voluntary contraction, and a maximal voluntary contraction. Both contractions were sustained for 10 s with a 2 min rest interval before, between and after the contractions. Muscle oxygenation was continuously monitored using our NIRS system placed over the quadriceps.

Participants

Able-bodied individuals (N=9) were recruited at university campuses (Table 1). All able-bodied had no history of cardiovascular problems, nor any neurological or orthopedic problems. Individuals with spinal cord injury (N=6) were recruited from current patients in the Spaulding Rehabilitation Hospital SCI exercise program for FES-rowing and were actively rowing on a weekly basis. All those with SCI were adults with spinal cord injury of American Spinal Association A-C at the neurological level of C6-L2 (Table 2). All subjects were medically stable, able to follow directions, able to reach sufficient leg joint range of motion to row, and able to respond to electrical stimulation of the quadriceps and hamstrings muscles. All subjects had a complete medical history and provided written informed consent. All procedures were approved by the Institutional Review Board at Spaulding Rehabilitation Hospital.

Exercise Protocol

All subjects performed a 10 min protocol, which involved 2 min of rest, 5 min of rowing, followed by an additional 3 min of rest. For the rest intervals, the individuals sat on the ergometer, with the knee angle set at 120°. The intensity of the rowing exercise was subject specific and intended to represent a moderate to high-intensity activity level of 70% of peak achievable workload for each individual [41]. The intensity level was estimated from the corresponding percentage of age-predicted heart rate for the able-bodied ((220 beats/min)-age), and from the maximum heart rate achieved during a prior maximal consumption oxygen test that has been performed for the exercise program for those with SCI [42]. For all the rowing tests, blood perfusion in the bone was measured continuously using our NIRS system by placing the probe head on the anterior side of the tibia.

A Concept2 ergometer was used for all the rowing tests. The adapted Concept2 ergometer allows those with SCI to perform functional electrical stimulation (FES) rowing, by simultaneously exercising the innervated upper body and the non-innervated lower body. FES-rowing has been previously established as an exercise intervention for those with SCI [34–36]. The adapted Concept2 ergometer has a high back seat unit with full shoulder harness that holds the rower, a telescopic leg stabilizers to prevent the paralyzed legs from moving in lateral direction and two springs underneath the rower rail that help the rower change direction of the movement [42]. A 4-channel electrical stimulator (Odstock, Salisbury, United Kingdom) was used to activate the quadriceps and hamstrings through surface skin electrodes placed over the muscle motor points, causing the legs to flex and extend. The Odstock stimulator was controlled by a trigger placed on the handle, allowing the rower to power their own leg muscles while pulling the handle. The stimulation intensity was set to pulses of 40 Hz with 400 μs pulse width, as is standard in the SCI rowing protocol.

All able-bodied individuals used the adapted Concept2 ergometer for the rowing tests. However, able-bodied individuals did not use the back seat, shoulder harness, telescopic leg stabilizer, and springs during rowing.

Data Analysis

NIRS measurements were made continuously during all rowing tests using our system. To minimize the influence of the transient periods between two different states (i.e. rest and rowing), we have used only 3 out of the 5 minutes of rowing (between the 1st and the 4th minute of rowing) and the last 2.5 minutes at the end of the exercise. We used the extended modified Beer-Lambert law (EMBLL) for a two-layer model to determine hemoglobin content changes in the bone from changes in light absorption [43–46]. The signal strength measured at detectors A and B at a single wavelength is given by:

$$I_A = I_0 \exp(-\mu_{a,1} L_{1,A} - G_{1,A} - \mu_{a,2} L_{2,A} - G_{2,A}), \quad (1)$$

$$I_B = I_0 \exp(-\mu_{a,1} L_{1,B} - G_{1,B} - \mu_{a,2} L_{2,B} - G_{2,B}), \quad (2)$$

where $\mu_{a,i}$ is the absorption coefficient for layer i; $L_{i,j}$ is the average optical pathlength of the photons in layer i that reach detector j and represents the product of the physical source-detector distance and a differential pathlength factor (DPF); and $G_{i,j}$ is the loss in signal due to scattering. A wavelength dependence was also explicitly assumed for each term in (1) and (2) but is not included in the symbols for clarity.

The optical density (OD) obtained for detectors A and B (at a single wavelength) is given by:

$$\mathrm{OD}_A = -\ln\frac{I_A}{I_0} = \mu_{a,1} L_{1,A} + G_{1,A} + \mu_{a,2} L_{2,A} + G_{2,A}, \quad (3)$$

$$\mathrm{OD}_B = -\ln\frac{I_B}{I_0} = \mu_{a,1} L_{1,B} + G_{1,B} + \mu_{a,2} L_{2,B} + G_{2,B}. \quad (4)$$

The dependence on G (due to scattering) is difficult to estimate and was eliminated by considering the difference between two measurements before and after exercise, and assuming that G was approximately constant over the relatively short timescale, i.e. that the changes in the detected signal were due to changes in absorption:

$$\Delta\mathrm{OD}_A = \mathrm{OD}_A(t_{\mathrm{after}}) - \mathrm{OD}_A(t_{\mathrm{before}}) = \Delta\mu_{a,1} L_{1,A} + \Delta\mu_{a,2} L_{2,A}, \quad (5)$$

$$\Delta\mathrm{OD}_B = \mathrm{OD}_B(t_{\mathrm{after}}) - \mathrm{OD}_B(t_{\mathrm{before}}) = \Delta\mu_{a,1} L_{1,B} + \Delta\mu_{a,2} L_{2,B}. \quad (6)$$

The effective pathlengths $L_{1,A}$, $L_{2,A}$, $L_{1,B}$, and $L_{2,B}$ in equations 1-6 were estimated using open source Monte Carlo photon modeling software [47], literature estimates of optical properties of skin and bone at different wavelengths [48], and the physical source-detector distance. The DPF factors were computed for each wavelength in the 700 – 900 nm range (Fig. 2). A refractive index of 1.34 and a scattering anisotropy factor (g) of 0.9 were used for both layers [48]. The absorbance and scattering coefficients for skin and bone were obtained at each wavelength, between 700 – 900 nm. The average absorbance coefficients for skin and bone were 0.026 mm^{-1} [49] and 0.216 mm^{-1} [50], respectively. The average scattering coefficients for skin and bone were 23.91 mm^{-1} [49] and 24.44 mm^{-1} [50], respectively. The thickness of the first layer representing the skin was assumed 1 - 3 mm [51], and of the second layer was assumed 37 - 39 mm [52]. The physical source-detector distance was 1 cm (detector A) and 2 cm (detector B), respectively. The desired chromophore concentration changes in each layer are obtained as follows. First, the change in the absorption coefficient at each wavelength for each layer ($\Delta\mu_{a,i}$) is estimated by solving the linear systems of equations:

$$\begin{bmatrix} \Delta\mu_{a,1} \\ \Delta\mu_{a,2} \end{bmatrix} = \boldsymbol{L}^{-1} \begin{bmatrix} \Delta\mathrm{OD}_A \\ \Delta\mathrm{OD}_B \end{bmatrix}, \quad (7)$$

with

$$\boldsymbol{L}=\begin{bmatrix} L_{1,A} & L_{2,A} \\ L_{1,B} & L_{2,B} \end{bmatrix}. \quad (8)$$

Then the change in concentration of the chromophores in each layer i (i.e., ΔO_2Hb_i and ΔHHb_i) is obtained by combining the $\Delta\mu_{a,i}$ values at all wavelengths and solving:

$$\begin{bmatrix} \Delta O_2Hb_i \\ \Delta HHb_i \end{bmatrix} = (\boldsymbol{E}^T\boldsymbol{E})^{-1}\boldsymbol{E}^T\Delta\boldsymbol{\mu}_{a,i}, \quad (9)$$

where $\boldsymbol{E}$ is a (number of wavelengths) × (number of chromophores) matrix whose columns are the known extinction coefficients of each chromophore; the superscript T denotes the transpose; and $\Delta\boldsymbol{\mu_{a,i}}$ is a column vector containing the $\Delta\mu_{a,i}$ values for all wavelengths for the ith layer. This solution is equivalent to a linear least-squares fit of the $\Delta\mu_{a,i}$ values. Established values were used for the extinction coefficients of oxygenated and deoxygenated hemoglobin [53]; in this wavelength range, the contribution of water and lipid chromophores is several orders of magnitude less than that of oxygenated and deoxygenated hemoglobin and thus it was not included.

Statistical analysis

Changes in O_2Hb and HHb concentrations in the tibia were assessed in able-bodied and SCI rowers using the two-layer EMBLL model presented between baseline and rowing exercise, and between baseline and post rowing. Changes in tHb concentration were assessed as the sum of the changes in O_2Hb and HHb concentration. Significant differences were determined using a one-sample t-test to determine changes from baseline during and after rowing. Differences in hemoglobin concentration between able-bodied rowers and SCI FES-rowers during rowing and post rowing were assessed using a two-tailed t-test. Statistical significance was set at 0.05 for all tests.

Validation study

Changes in O_2Hb and HHb concentrations in the quadriceps group during sustained muscle contractions were assessed using a simplified one-layer model to be directly comparable to previous studies and the output of commercial systems. Specifically, we computed

$$\begin{bmatrix} \Delta O_2Hb * L \\ \Delta HHb * L \end{bmatrix} = (\boldsymbol{E}^T\boldsymbol{E})^{-1}\boldsymbol{E}^T\Delta\boldsymbol{OD}_B, \quad (10)$$

where $\Delta\boldsymbol{OD_B}$ is a column vector containing the ΔOD_B values measured at all wavelengths. To be consistent with the frequently used convention [54,55], we adopted the μMcm form of the solution for these experiments only (i.e. solving for the product of the optical pathlength

and the changes in concentration in μMcm). Changes in total hemoglobin content (tHb) concentration were assessed as the sum of the changes in O_2Hb and HHb concentration.

Results

Validation: Muscle response during exercise

During sustained isometric exercise at 30% maximum voluntary contraction and 100% maximum voluntary contraction, there was a decrease in total hemoglobin content in the quadriceps muscles, with a rapid increase in total hemoglobin at the end of the contraction (Fig. 3). During isometric contractions, intermuscular pressure increases, compressing the microcirculation vessels and restricting arterial inflow to the muscle, resulting in a rapid ejection of venous blood [56]. Studies using commercially available NIRS devices have found similar behavior in changes in total hemoglobin in both sustained and intermittent exercise in the quadriceps and biceps muscles [40,54,57]. This demonstrated that our device is able to detect comparable changes in blood perfusion in skeletal muscle.

Acute changes in blood perfusion in bone in response to exercise

In able-bodied individuals, the intensity of the scattered light measured across the tibia declined both during rowing, as well as post rowing (Fig. 4). An increase in blood content (chromophore concentration) results in more light being absorbed and thus a decrease in diffused light measured by the detectors. Therefore, the decrease in light intensity for the two detectors indicates an increase in blood perfusion both in skin and bone. The oscillations in the signal measured during the rowing interval was due to slight changes in coupling of the light from the skin surface into the optical fibers during the rowing cycle (we note that this was not evident before or after rowing where the individual was stationary).

When an inert material (i.e rubber eraser) was placed between the leg and the holder of the NIRS device during the rowing exercise, no change in light intensity was measured for either of the two detectors during rowing or post rowing (Fig. 5). The oscillation during the rowing interval was not evident because the material was rigid and light coupling was not disturbed. Overall, this indicates that the light intensity trends measured during rowing (Fig. 4) were due to physiological changes in blood perfusion in the skin and bone and were not, for example, movement of the probe position over the course of the experiment.

We used the full measured spectra to measure changes in hemoglobin concentrations (in μM) during and after exercise as described above. As a group, in able-bodied rowers, there was an increase in deoxygenated blood (HHb) concentration in the tibia during rowing ($p=0.02$), with no changes in either oxygenated (O_2Hb) or total hemoglobin (tHb) concentration (Fig. 6). We note that data from 3 minutes of the rowing interval was averaged in each case, which mitigated the oscillations in the signal. Post exercise, able-bodied rowers had an almost significant increase in tHb concentration ($p=0.06$). A power analysis indicated that to maintain a statistical significance of 0.05, an additional of 8 subjects would be needed to find a significant increase in tHb concentration post rowing. The immediate increase in tHb post rowing resulted mainly due to an increase in HHb ($p=0.02$), while no change in O_2Hb concentration was found.

In those with SCI, there was an almost significant decrease in O_2Hb concentration in the tibia during FES-rowing ($p=0.06$), with no changes in HHb and tHb concentrations (Fig. 7). A power analysis indicated that to maintain a statistical significance of 0.05, an additional of 8 subjects would be needed to find a significant decrease in O_2Hb concentration during rowing. Post FES-rowing, those with SCI showed no change in either O_2Hb, HHb, or tHb concentration.

Thus, with rowing, deoxygenated blood increased in able-bodied individuals during and after rowing. However, in FES-rowing, those with SCI showed only a decrease in O_2Hb during rowing, with no significant changes in tHb post FES-rowing.

During rowing, able-bodied rowers had a greater change in HHb concentration than SCI rowers ($p=0.03$ HHb). Similarly, after rowing, able-bodied rowers had a greater change in HHb concentration compared to SCI FES-rowers ($p=0.03$ HHb).

Discussion

In this study, we built, tested, and validated a custom NIRS instrument to monitor changes in hemoglobin content in the human tibia with rowing exercise. Our preliminary investigations here showed that our instrument provides a similar response with respect to muscle oxygenation during quadriceps isometric contraction as commercially available NIRS systems. The total hemoglobin content found during 30% and 100% maximum voluntary contractions has similar behavior and order of magnitude to that found during maximum brachialis contractions in the arm [40,54]. Additionally, the experiments conducted with inert materials showed that our system indeed captures a physiological response in blood perfusion in the tibia.

As we discussed, NIRS measurements require firm coupling of light sources and detectors to the skin surface, and therefore are sensitive to both positioning and subject motion. The positioning of the apparatus on the tibial bone will introduce inter-subject variability related to placement, tissue properties, and anatomical variability. Noisy fluctuations were evident during the rowing intervals where the motion periodically altered light-tissue coupling, resulting in oscillations in the signal. We minimized this by ensuring close interface between the detector fibers and the leg, and by averaging the data over the entire interval. Despite this, we attribute some of the higher observed variability in chromophore concentrations in both groups during rowing compared to post exercise (Fig. 5 and Fig. 6) to this effect. Finally, to minimize variability due to leg positioning, all measurements pre- and post-exercise were taken in the same position (knee angle set to 120 deg) for all subjects. We discarded all trials that suggested possible shifting of the apparatus anytime during the test period.

We also quantified changes in blood content in the tibia with rowing in able-bodied and in individuals with SCI. In able-bodied individuals, total blood content in the tibia increases immediately after exercise. This response is quantified by an increase in deoxygenated hemoglobin during rowing and an increase in total hemoglobin content post exercise due primarily to a further increase in deoxygenated hemoglobin. In the SCI individuals, the

response to FES-rowing was characterized only by a decrease in oxygenated hemoglobin during rowing, but no other changes in blood content during or post exercise were found. This result is not surprising given the impaired peripheral circulation seen in individuals with SCI [32,33]. Our results are also in agreement with the slower hemoglobin recovery time post cuff inflation response seen by Khakha *et al.* [29] in SCI compared to able-bodied. This suggests that in individuals with SCI using FES-driven muscle activation, the level of activity is not sufficient to result in an increase in blood content as seen in the able-bodied population.

One of the limitations of this study is that our results could not be directly validated with literature values. To date, there are no established measurements of acute changes in total blood content in the human bone (which was precisely the motivation for developing this sensor) and thus it is difficult to quantitatively validate our results. The lack of comparable data in the literature underscores the high potential value of the NIRS technique to the field. Our estimates of hemoglobin concentration depend on different geometrical (i.e. skin thickness) and optical properties (i.e. skin and bone absorption and scattering coefficients). To assess the influence of different geometrical parameters, we varied the skin tissue layer between 1 mm and 3 mm. The resulting concentrations were within the standard error of our model. To assess the influence of different optical parameters, we varied the chosen absorption and scattering parameters for both skin and bone by ± 25%. Additionally, we considered a new set of optical parameters for skin that reflect the dermis layer (absorbance 0.025 mm^{-1} [58,59] and scattering 16.84 mm^{-1} [59]) and for bone (absorbance 0.015 mm^{-1} [60] and scattering 19.66 mm^{-1} [60]). As in the case of skin thickness, the resulting concentrations using the different optical properties were within the standard error of our model. Though the magnitude of the change in oxy-deoxy hemoglobin is sensitive to the skin thickness and optical properties, the overall conclusions (increase/decrease in blood) are robust.

This study extends previous work that demonstrated the potential of NIRS measurements of blood in tibial cortical bone using cuff inflation in a single subject[22] and in different superficial bones using a single-layer system[25]. In this work we demonstrate that NIRS is able to measure significant physiological changes in blood perfusion during exercise in a cohort of able-bodied individuals. Not surprisingly exercise did not produce a change in blood in bone in SCI subjects. We extend previous work using two detectors in our system and a two-layer model that minimizes the influence of the skin tissue, which is highly perfused and may cause significant artifact. Whereas previous studies used single wavelength light, we used a broadband light source, which will allow measurement of additional chromophore content such as water or lipids in future studies.

To conclude, the current study demonstrates the feasibility of using NIRS to detect changes in hemoglobin concentration in the human cortical bone. We have demonstrated that NIRS allows non-invasive monitoring of blood content changes in the human bone. Future work will use this technology in clinical applications such as stress fracture detection, where there is value in providing real-time in-clinic measurements of blood perfusion in bone.

Supplementary Material

Refer to Web version on PubMed Central for supplementary material.

Acknowledgments

This study was supported by a Tier 1 Northeastern University Research Funding and by the National Institute of Health (R01 HL117037). We thank all our subjects for their participation.

References

1. McCarthy I. The Physiology of Bone Blood Flow: A Review. J Bone Jt Surg. 2006; 88:4–9.
2. Brandi ML, Collin-Osdoby P. Vascular Biology and the Skeleton. J Bone Miner Res. 2006; 21:183–192. [PubMed: 16418774]
3. Gerber HP, et al. VEGF couples hypertrophic cartilage remodeling, ossification and angiogenesis during endochondral bone formation. Nat Med. 1999; 5:623–628. [PubMed: 10371499]
4. Lafage-Proust MH, et al. Assessment of bone vascularization and its role in bone remodeling. BoneKEy Rep. 2015; 4:662. [PubMed: 25861447]
5. Lewinson D, Silbermann M. Chondroclasts and endothelial cells collaborate in the process of cartilage resorption. Anat Rec. 1992; 233:504–514. [PubMed: 1626710]
6. Roach HI, Baker JE, Clarke NM. Initiation of the bony epiphysis in long bones: chronology of interactions between the vascular system and the chondrocytes. J Bone Miner Res Off J Am Soc Bone Miner Res. 1998; 13:950–961.
7. Driessens M, Vanhoutte PM. Vascular reactivity of the isolated tibia of the dog. Am J Physiol. 1979; 236:H904–908. [PubMed: 443457]
8. McCarthy ID, Yang L. A distributed model of exchange processes within the osteon. J Biomech. 1992; 25:441–450. [PubMed: 1583022]
9. Zhu J, et al. Reduction of Longitudinal Vertebral Blood Perfusion and Its Likely Causes: A Quantitative Dynamic Contrast-enhanced MR Imaging Study of a Rat Osteoporosis Model. Radiology. 2016; 152006doi: 10.1148/radiol.2016152006
10. Heymann MA, Payne BD, Hoffman JI, Rudolph AM. Blood flow measurements with radionuclide-labeled particles. Prog Cardiovasc Dis. 1977; 20:55–79. [PubMed: 877305]
11. Prinzen FW, Glenny RW. Developments in non-radioactive microsphere techniques for blood flow measurement. Cardiovasc Res. 1994; 28:1467–1475. [PubMed: 8001033]
12. Rudnick-Glick S, Corem-Salkmon E, Grinberg I, Yehuda R, Margel S. Near IR fluorescent conjugated poly(ethylene glycol)bisphosphonate nanoparticles for in vivo bone targeting in a young mouse model. J Nanobiotechnology. 2015; 13:80. [PubMed: 26577112]
13. Ferrari M, Quaresima V. A brief review on the history of human functional near-infrared spectroscopy (fNIRS) development and fields of application. NeuroImage. 2012; 63:921–935. [PubMed: 22510258]
14. Boas DA, Elwell CE, Ferrari M, Taga G. Twenty years of functional near-infrared spectroscopy: introduction for the special issue. NeuroImage. 2014; 85, Part 1:1–5. [PubMed: 24321364]
15. Leff DR, et al. Assessment of the cerebral cortex during motor task behaviours in adults: a systematic review of functional near infrared spectroscopy (fNIRS) studies. NeuroImage. 2011; 54:2922–2936. [PubMed: 21029781]
16. Torricelli A, et al. Time domain functional NIRS imaging for human brain mapping. NeuroImage. 2014; 85, Part 1:28–50. [PubMed: 23747285]
17. Wolf M, Ferrari M, Quaresima V. Progress of near-infrared spectroscopy and topography for brain and muscle clinical applications. J Biomed Opt. 2007; 12:062104. [PubMed: 18163807]
18. Binzoni T, et al. Human tibia bone marrow blood perfusion by non-invasive near infrared spectroscopy: a new tool for studies on microgravity. J Gravitational Physiol J Int Soc Gravitational Physiol. 2002; 9:183–184.

19. Binzoni T, et al. Blood volume and haemoglobin oxygen content changes in human bone marrow during orthostatic stress. J Physiol Anthropol. 2006; 25:1–6. [PubMed: 16617202]
20. Farzam P, et al. Noninvasive characterization of the healthy human manubrium using diffuse optical spectroscopies. Physiol Meas. 2014; 35:1469–1491. [PubMed: 24901605]
21. Binzoni T, et al. Human tibia bone marrow: defining a model for the study of haemodynamics as a function of age by near infrared spectroscopy. J Physiol Anthropol Appl Human Sci. 2003; 22:211–218.
22. Aziz SM, et al. A near infrared instrument to monitor relative hemoglobin concentrations of human bone tissue in vitro and in vivo. Rev Sci Instrum. 2010; 81:043111. [PubMed: 20441329]
23. Farzam P, Zirak P, Binzoni T, Durduran T. Pulsatile and steady-state hemodynamics of the human patella bone by diffuse optical spectroscopy. Physiol Meas. 2013; 34:839–857. [PubMed: 23859825]
24. Näslund JE, Näslund S, Lundeberg E, Lindberg LG, Lund I. Bone blood flow is influenced by muscle contractions. J Biomed Sci Eng. 2011; 04:490.
25. Sekar SKV, et al. In Vivo, Non-Invasive Characterization of Human Bone by Hybrid Broadband (600-1200 nm) Diffuse Optical and Correlation Spectroscopies. PLOS ONE. 2016; 11:e0168426. [PubMed: 27997565]
26. Heinonen I, et al. Bone blood flow and metabolism in humans: Effect of muscular exercise and other physiological perturbations. J Bone Miner Res. 2013; 28:1068–1074. [PubMed: 23280932]
27. Stabley JN, Moningka NC, Behnke BJ, Delp MD. Exercise training augments regional bone and marrow blood flow during exercise. Med Sci Sports Exerc. 2014; 46:2107–2112. [PubMed: 24658222]
28. Khakha RS, et al. Differences in the Reactive Hyperemia Response of Bone in Able Bodied and Spinal Injured Persons Using Near Infrared Spectroscopy. Orthop Proc. 2006; 88–B:305–305.
29. McCarthy I. Application of Near Infrared Spectroscopy in the Assessment of Bone Perfusion. Orthop Proc. 2012; 94–B:36–36.
30. Faghri PD, Yount JP, Pesce WJ, Seetharama S, Votto JJ. Circulatory hypokinesis and functional electric stimulation during standing in persons with spinal cord injury. Arch Phys Med Rehabil. 2001; 82:1587–1595. [PubMed: 11689980]
31. Minaire P, Edouard C, Arlot M, Meunier PJ. Marrow changes in paraplegic patients. Calcif Tissue Int. 1984; 36:338–340. [PubMed: 6432298]
32. Olive JL, McCully KK, Dudley GA. Blood flow response in individuals with incomplete spinal cord injuries. Spinal Cord. 2002; 40:639–645. [PubMed: 12483497]
33. West CR, Alyahya A, Laher I, Krassioukov A. Peripheral vascular function in spinal cord injury: a systematic review. Spinal Cord. 2013; 51:10–19. [PubMed: 23184028]
34. Davoodi R, Andrews BJ, Wheeler GD, Lederer R. Development of an indoor rowing machine with manual FES controller for total body exercise in paraplegia. IEEE Trans Neural Syst Rehabil Eng Publ IEEE Eng Med Biol Soc. 2002; 10:197–203.
35. Davoodi R, Andrews BJ. Fuzzy logic control of FES rowing exercise in paraplegia. IEEE Trans Biomed Eng. 2004; 51:541–543. [PubMed: 15000386]
36. Laskin JJ, et al. Electrical stimulation-assisted rowing exercise in spinal cord injured people. A pilot study. Paraplegia. 1993; 31:534–541. [PubMed: 8414639]
37. Hamaoka T, McCully KK, Niwayama M, Chance B. The use of muscle near-infrared spectroscopy in sport, health and medical sciences: recent developments. Phil Trans R Soc A. 2011; 369:4591–4604. [PubMed: 22006908]
38. Hamaoka T, McCully KK, Quaresima V, Yamamoto K, Chance B. Near-infrared spectroscopy/imaging for monitoring muscle oxygenation and oxidative metabolism in healthy and diseased humans. J Biomed Opt. 2007; 12:062105. [PubMed: 18163808]
39. Katayama K, Yoshitake Y, Watanabe K, Akima H, Ishida K. Muscle deoxygenation during sustained and intermittent isometric exercise in hypoxia. Med Sci Sports Exerc. 2010; 42:1269–1278. [PubMed: 20019635]
40. Muthalib M, Millet GY, Quaresima V, Nosaka K. Reliability of near-infrared spectroscopy for measuring biceps brachii oxygenation during sustained and repeated isometric contractions. J Biomed Opt. 2010; 15:017008. [PubMed: 20210482]

41. Centers for Disease Control and Prevention. [Accessed: 10th January 2017] Target Heart Rate and Estimated Maximum Heart Rate |Physical Activity| CDC. Available at: https://www.cdc.gov/physicalactivity/basics/measuring/heartrate.htm
42. Taylor JA, Picard G, Widrick JJ. Aerobic Capacity With Hybrid FES Rowing in Spinal Cord Injury: Comparison With Arms-Only Exercise and Preliminary Findings With Regular Training. PM&R. 2011; 3:817–824. [PubMed: 21944299]
43. Delpy DT, et al. Estimation of optical pathlength through tissue from direct time of flight measurement. Phys Med Biol. 1988; 33:1433. [PubMed: 3237772]
44. Hiraoka M, et al. A Monte Carlo investigation of optical pathlength in inhomogeneous tissue and its application to near-infrared spectroscopy. Phys Med Biol. 1993; 38:1859. [PubMed: 8108489]
45. Şayli Ö, Akın A. Two-distance partial pathlength method for accurate measurement of muscle oxidative metabolism using fNIRS. 2006; 6084:60840O–60840O. 8.
46. Wilson BC, Jacques SL. Optical reflectance and transmittance of tissues: principles and applications. IEEE J Quantum Electron. 1990; 26:2186–2199.
47. Fang Q, Boas DA. Monte Carlo Simulation of Photon Migration in 3D Turbid Media Accelerated by Graphics Processing Units. Opt Express. 2009; 17:20178. [PubMed: 19997242]
48. Jacques SL. Optical properties of biological tissues: a review. Phys Med Biol. 2013; 58:R37–61. [PubMed: 23666068]
49. Bashkatov AN, Genina EA, Tuchin VV. Optical Properties of Skin, Subcutaneous, and Muscle Tissues: A Review. J Innov Opt Health Sci. 2011; 04:9–38.
50. Alexandrakis G, Rannou FR, Chatziioannou AF. Tomographic bioluminescence imaging by use of a combined optical-PET (OPET) system: a computer simulation feasibility study. Phys Med Biol. 2005; 50:4225. [PubMed: 16177541]
51. Yalcin E, Akyuz M, Onder B, Unalan H, Degirmenci I. Skin thickness on bony prominences measured by ultrasonography in patients with spinal cord injury. J Spinal Cord Med. 2013; 36:225–230. [PubMed: 23809593]
52. Patterson J, et al. Cortical Bone Thickness of the Distal Part of the Tibia Predicts Bone Mineral Density. J Bone Joint Surg Am. 2016; 98:751–760. [PubMed: 27147688]
53. Prahl, S. [Accessed: 29th January 2017] Optical Absorption of Hemoglobin. Available at: http://omlc.org/spectra/hemoglobin/
54. Felici F, et al. Biceps brachii myoelectric and oxygenation changes during static and sinusoidal isometric exercises. J Electromyogr Kinesiol Off J Int Soc Electrophysiol Kinesiol. 2009; 19:e1–11.
55. Muthalib M, Millet GY, Quaresima V, Nosaka K. Reliability of near-infrared spectroscopy for measuring biceps brachii oxygenation during sustained and repeated isometric contractions. J Biomed Opt. 2010; 15:017008–017008. 8. [PubMed: 20210482]
56. Sjøgaard G, Kiens B, Jørgensen K, Saltin B. Intramuscular pressure, EMG and blood flow during low-level prolonged static contraction in man. Acta Physiol Scand. 1986; 128:475–484. [PubMed: 3788624]
57. de Ruiter CJ, de Boer MD, Spanjaard M, de Haan A. Knee angle-dependent oxygen consumption during isometric contractions of the knee extensors determined with near-infrared spectroscopy. J Appl Physiol Bethesda Md 1985. 2005; 99:579–586.
58. Jacques, SL. [Accessed: 8th February 2017] Skin Optics. 1998. Available at: http://omlc.org/news/jan98/skinoptics.html
59. Bashkatov AN, Genina EA, Kochubey VI, Tuchin VV. Optical properties of human skin, subcutaneous and mucous tissues in the wavelength range from 400 to 2000 nm. J Phys Appl Phys. 2005; 38:2543.
60. Bashkatov AN, Genina EA, Kochubey VI, Tuchin VV. Optical properties of human cranial bone in the spectral range from 800 to 2000 nm. 2006; 6163:616310–616310. 11.

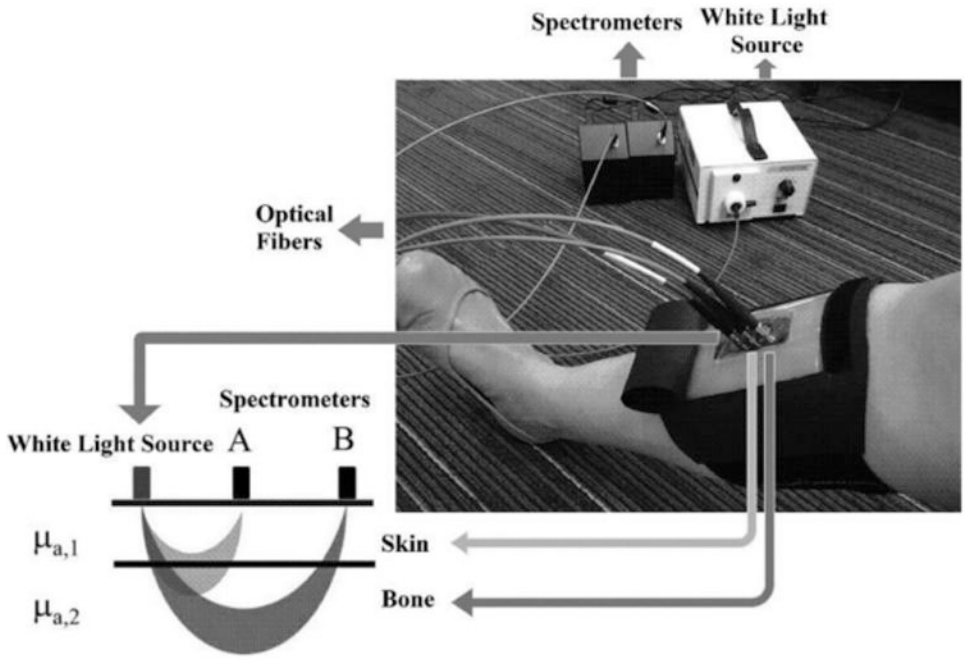

Figure 1.
NIRS device for measuring blood perfusion in tibia.

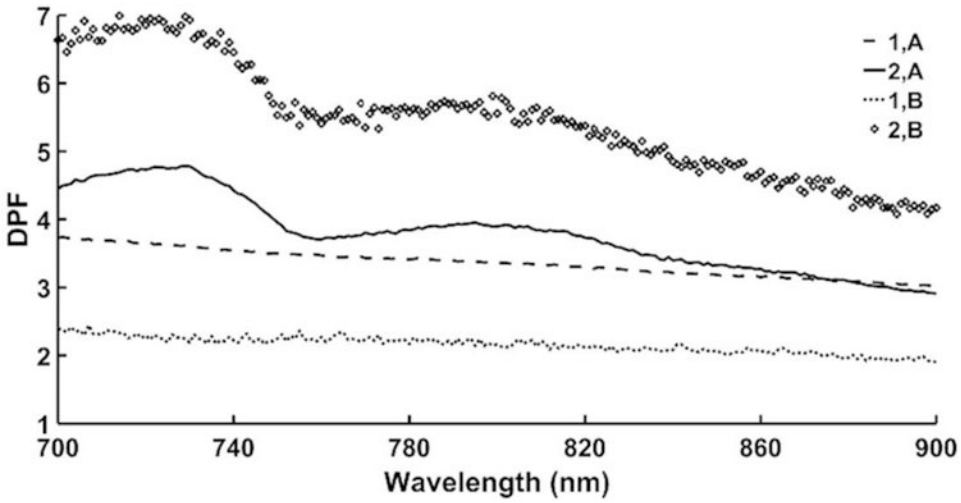

Figure 2.

The computed differential pathlength factors (DPF) using open source Monte Carlo photon modeling software for the considered wavelength range of 700 – 900 nm. (Notations: 1, A represents the light absorbed by the 1st layer that reaches detector A; 2, A represents the light absorbed by the 2nd layer that reaches detector A; 1, B represents the light absorbed by the 1st layer that reaches detector B; 2, B represents the light absorbed by the 2nd layer that reaches detector B.)

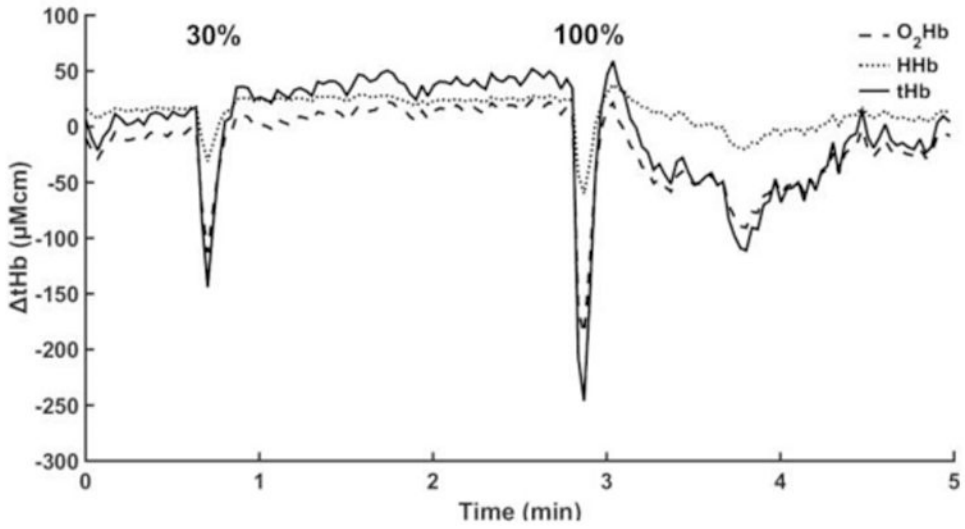

Figure 3.

Changes in total hemoglobin concentration (μM*cm) in the muscle during sustained quadriceps contraction in an able-bodied individual. The two responses represent sustained quadriceps contraction at 30% and 100% of maximum voluntary contraction.

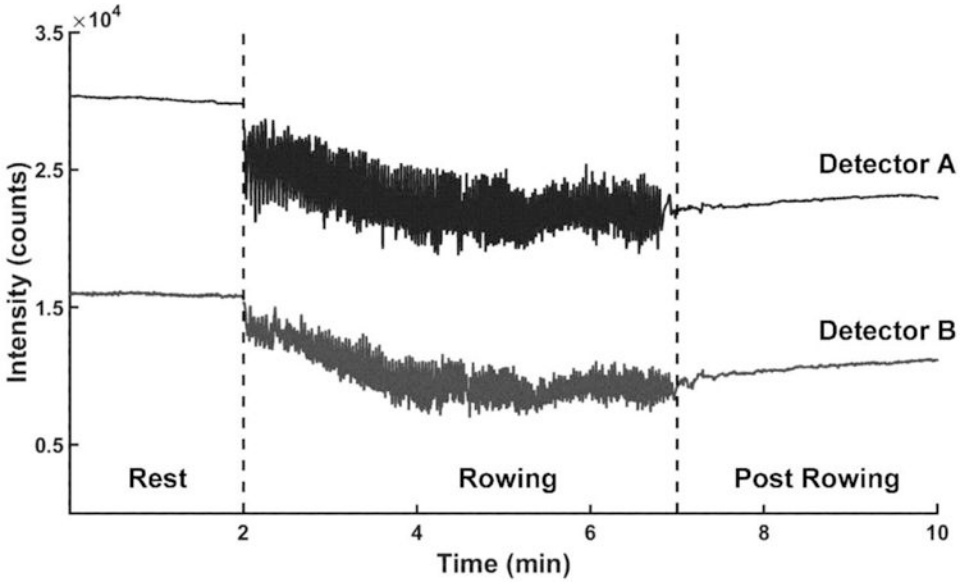

Figure 4.

Intensity of light absorbed by the two detectors for a representative able-bodied individual during a rowing exercise (NIRS probe placed on the skin over the tibia; source-detector A distance = 1 cm; source-detector B distance = 2 cm; Light intensity spectrum at wavelength λ = 810 nm).

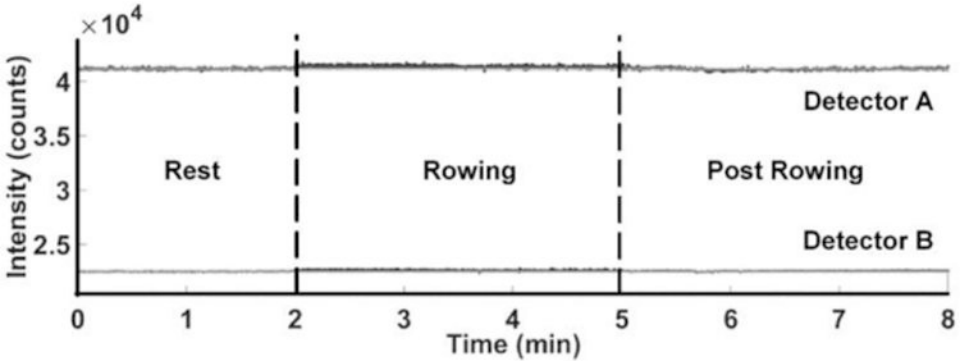

Figure 5.

Intensity of light absorbed by the two detectors for an able-bodied individual during a rowing exercise, when an inert material (i.e. rubber eraser) is placed between the leg and NIRS probe.

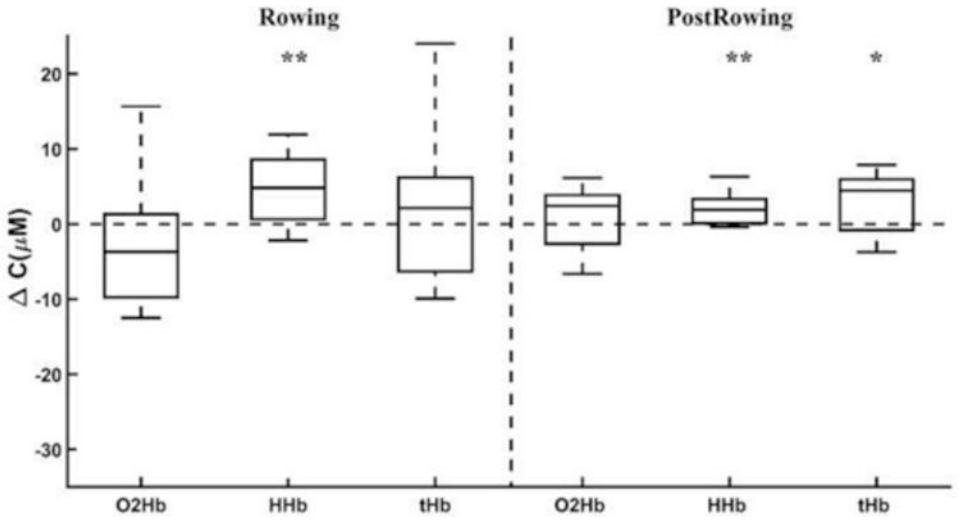

Figure 6.

Changes in O_2Hb, HHb, and tHb in the tibia in able-bodied individuals during rowing and post rowing (* $p<0.1$, ** $p<0.05$ different from zero). For each concentration, boxplots show the median and the maximum and minimum non-outliers (whiskers).

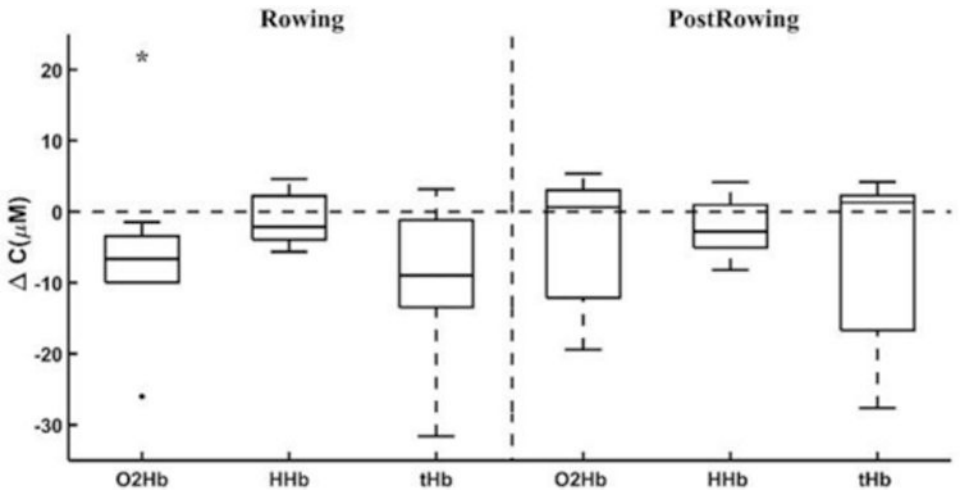

Figure 7.

Changes in O_2Hb, HHb, and tHb in the tibia in those with SCI during FES-rowing and post FES-rowing (* $p<0.1$, ** $p<0.05$). For each concentration, boxplots show the median, the maximum and minimum non-outliers (whiskers), and outliers (+ points).

Table 1

Able-bodied subjects' characteristics.

Participant	Age (y)	Weight (kg)	Height (m)	Sex
1	23	78.02	1.803	F
2	22	66.68	1.727	F
3	27	62.14	1.676	F
4	22	60.00	1.700	F
5	20	65.57	1.626	M
6	20	65.77	1.803	M
7	21	74.00	1.800	M
8	24	86.18	1.778	M
9	40	68.00	1.727	M

Table 2

Spinal cord injured subjects' characteristics.

Participant	Lesion Level	ASIA Classification	Age (y)	Time Since Injury (y)	Weight (kg)	Height (m)	Sex
1	T4	A	43	20	54.59	1.803	M
2	T5	N/A	27	4	97.27	1.778	M
3	C6	A	38	15	87.36	1.702	M
4	T2	N/A	37	24	86.23	1.727	M
5	L2	A	27	9	61.27	1.626	F
6	C6	A	33	9	59.06	1.524	F

ASIA = American Spinal Injury Association